Bionatura
Latin American Journal of Biotechnology and Life Sciences

Bionatura Issue 1 Vol 8 No 1 2023

Article

Evaluation of the Inhibitory Activity of *Syzygium aromaticum* Extract -Chitosan Nanoparticles Against Biofilm Formation of *Klebsiella pneumonia*

Hussein Ali shaghati[1,*], Emad Hamdi Jassim[2], Labib A. Kadhim AL-Zubaidi [3]
[1] Genetic engineering and biotechnology institute, University of Baghdad. Iraq ; hussein.ali1300a@ige.uobaghdad.edu.iq .ORCID 0000-0002-3542-2268
[2] Genetic engineering and biotechnology institute, University of Baghdad. Iraq emadhamdi@ige.uobaghdad.edu.iq
[3] Environment & Water Directorate/ Ministry of Science& Technology, Baghdad. Iraq.
*Correspondence: hussein.ali1300a@ige.uobaghdad.edu.iq
Available from: http://dx.doi.org/10.21931/RB/CSS/2023.08.01.71

Abstract: The increasing resistance of *Klebsiella pneumoniae* to antibiotics has led to difficulties in treating infections due to its virulence factors. As one of its major pathogenic factors, this opportunistic pathogen may develop a thick biofilm coating, allowing the bacteria to attach to living or nonliving surfaces and promote drug resistance. Searching for therapeutic alternatives from a plant source that was safe and effective in treating this multi-drug-resistant bacteria was necessary. In this concept, *Syzygium aromaticum* extract (SAE) is used to combat *K. pneumonia*. The extract was confirmed by GC-MS and loaded onto chitosan nanoparticles (SACSNPs). The SACSNPs were prepared by the ionic gelation method with tripolyphosphate (TPP). And then characterized using UV-vis, FTIR, AFM, SEM, and XRD techniques. The *K. pneumonia* isolates were obtained and identified using the VITEK-2 system. The MIC of SAE and SACSNPs were confirmed using a 96-well resazurin-aided microdilution method, which was 6.25 µg/ml for SACSNPs and 75.5 µg/ml for SAE. The inhibitory activity using sub-MIC of analytical substances was determined by measuring the optical density using a microplate reader with a 96-well plate and 0.1% crystal violet dye. The results show that the *S. aromaticum* extract loaded with chitosan nanoparticles has higher inhibitory activity against the biofilm formation of *K. pneumonia* than the *S. aromaticum* extract.

Keywords: Chitosan nanoparticles, *S. aromaticum*, *K. pneumonia*, Biofilm, GC-MS, resazurin, XRD.

Introduction

K. pneumoniae is a member of the Enterobacteriaceae family and is one of the pathogenic bacteria that cause urinary tract infections. It is also susceptible to antibiotic resistance, which limits its treatment options [1]. Biofilm producers of these bacteria have a high level of antibiotic resistance, leading to complications in the treatment of infections [2]. Herbal and naturally occurring substances have been utilized for medicinal purposes since ancient times when stories, traditions, and literature were used to identify plants that might relieve pain and treat diseases [3]. These plants produce various bioactive chemicals that are effective

antibacterial agents against various pathogenic organisms. Some bioactive compounds derived from traditional plants can reverse antibiotic resistance and improve the synergetic effect of already available antibiotics [4]. The dried flower buds of Syzygium aromaticum (clove) from the Myrtaceae family are a traditional spice used for food preservation and have various therapeutic benefits [5]. It is a rich source of phenolic compounds, including eugenol and eugenol acetate, and it has much potential in the pharmaceutical, cosmetic, food, and agricultural industries [6]. Eugenol (4-allyl-2-methoxyphenol) is a natural phenol present in the essential oils of plants, including cloves, walnuts, nutmeg, and cinnamon. It has been shown to have many therapeutic properties such as anti-inflammatory, anesthetic, analgesic, antipyretic, antiplatelet, antibacterial, anti-anaphylactic, anti-depressant, anti-convulsant, anti-hyperglycemic, antifungal, and antiviral properties [7]. The antibacterial effect of eugenol is based on its ability to kill bacteria by penetrating the bacterial nucleic acid and cytoplasmic membranes, resulting in cell wall integrity loss, nucleic acid damage, and increased cell wall permeability.

Nanotechnology has recently received wide attention from researchers because of its unique properties that distinguish it in various fields, including its use as a drug carrier [8] because natural biopolymers increase biodegradability, enhanced stability, biocompatibility, gradual drug release capability, higher stability, most excellent antibacterial activity, and low toxicity of the component materials after encapsulation [9]. The most significant advantages of nanoparticles employed as medication carriers are excellent stability, high carrier capacity, ease of accepting hydrophilic and hydrophobic molecules, and various delivery methods, including oral and inhalation [10]. Among the several biopolymers, chitosan is ideal for encapsulation because of its biodegradability, biocompatibility, and low toxicity [11]. Chitosan nanoparticles (CSNPs) have a wide range of applications as nanocarriers for encapsulating drugs or active chemicals, transporting them to a specific location, and then releasing them in a controlled manner [12]. Nanoparticles (NPs) produced from chitosan and its derivatives have a positive surface charge and high biocompatibility, allowing them to bind to mucus membranes and slowly release the therapeutic content [13]. This study aimed to create a novel, effective and safe medication from SAE loaded with chitosan nanoparticles and evaluate its inhibitory impact on the biofilm formation of Klebsiella pneumoniae, which causes urinary tract infections.

Materials and methods

Preparation of S. aromaticum extract (SAE)

The flower buds of S. aromaticum were purchased from the local markets of Baghdad. The air-dried ground plant material was extracted according to [14] 150 g from the plant with the 500 ml solvent aqueous methanol (methanol: water, 80 % v/v) for 8 hours under Soxhlet on a water bath. The extracts were concentrated using a rotary evaporator and dried.

GC-MS analysis of SAE

Chemical components of the SAE were identified by an Agilent (7820A) GC Mass Spectrometer, Injection volume 1µl of the sample, by maintaining the oven temperature at 70˚C and the Injector Temperature: 250 ˚C. Time amounted to about 34 minutes; the chemical constituents of SAE were identified by comparing the chromatogram results and reference retention time using the Wiley mass spectra library [15].

Biosynthesis of SAE/chitosan nanoparticles (SACSNPs)

The preparation of SACSNPs as reported by [16] Briefly, chitosan nanoparticles were obtained through an ionic gelation pathway by using TPP, 5 mg/ml of 5% SAE was dissolved in acetic acid solution 1% w/v and mixed until the solution was clear then, Tripolyphosphate (TPP) solution was added to CS- SAE solution with ratios; 1: 2.5 (w/w %) with continuous stirring at ambient temperature for 6h. The production of CS- SAE /TPP nanoparticles started via the TPP-initiated ionic gelation mechanism. These nanoparticles were separated and washed several times, then the supernatant layer was removed, and the precipitate was re-suspended in water and dried.

Determination of eugenol compound in SAE and SACSNPs. Using HPLC technique

High-performance liquid chromatography (HPLC) analysis was conducted to determine the concentration of eugenol in the SAE and SACSNPs using the method adapted from [17]. Using SYKAMN HPLC system (Germany) equipped with a C18-ODS column (250 × 4.6 mm, 5 µm). Samples (100 µl) were injected into the system. The mobile phase comprised 95% acetonitrile + 0.01% trifluoracetic acid (solvent A) and 5% acetonitrile + 0.01% trifluoracetic acid (solvent B) at 1 ml/min. The detection of phenolic compounds was carried out with a UV-visible detector at 278 nm. Eugenol was quantified using a calibration curve and peak area measurements. The concentrations are calculated according to equation (1) [18]

The concentration of sample=concentration of std. *Area sample/Area std……. (1)

Characterization of SAE/Chitosan nanoparticles (SACSNPs)

Uv-vis Spectroscopy

UV-VIS double beam spectrophotometers were used to measure the absorbance spectra of the SACSNPs solution. The absorption was calculated using 200-800nm [19].

Fourier-transform infrared spectroscopy analysis FTIR

The characterization of functional groups on the surface of SACSNPs and SAE was investigated by FTIR analysis (Shimadzu), and the spectra were scanned at a resolution of 4 cm^{-1} in the range of 4000 - 400 cm^{-1}. The samples were processed according to standard methods [20].

Atomic force microscope analysis AFM

The surface morphology of SACSNPs was visualized by Atomic Force Microscope Contact mode under normal atmospheric conditions. Analysis was carried out according to the standard procedure as described by [21].

Scanning electron microscopy analysis SEM

A scanning electron microscope (SEM) was employed to analyze the morphology of the formed nanoparticles. SACSNPs were morphologically characterized using a Brucker Scanning Electron Microscope. The samples were prepared according to standard methods. [22].

X-Ray Diffraction XRD

The crystallinity of the prepared nanoparticles was determined using an X-ray diffractometer. The pattern of CS & SACSNP samples was analyzed using an X-ray diffractometer with Cu- Kα radiation as an anode at the wavelength (0.154060 nm) and a detector operating at (40 kV) and a current of (30 mA). In a fixed time mode at room temperature, the XRD pattern was observed in the 2θ range of 10° to 80°[23].

Samples collection and identification

Fifty K. pneumonia isolates were collected from two Iraqi hospitals, Al Karama and Ghazi Hariri Hospital, from patients suffering from UTI. All isolates were cultured on MacConkey and Blood agar and incubated at 37°C for 18-24 hours according to standard methods [24]. For identification of isolates based on the morphology of colonies, the isolates were inoculated on CHROMagar and incubated at 37°C for 18-24 hours [25]. The Vitek-2 system test was performed to identify K. pneumonia isolates.

Determination of MIC using the microtiter plate method MTP

The MIC and MBC of SAE and SACSNPs were assessed against Gram-negative K. pneumonia. Using a 96-well microtiter plate assisted the resazurin dye in Mueller-Hinton broth (MHB) as reported by [26].

Detection of inhibitory efficacy of SAE and SACSNPs against biofilm formation of K. pneumonia

The microtiter plate (MTP) assay is a qualitative technique that uses a microplate reader to determine an agent's effectiveness against biofilm formation. The sub-MIC obtained from the previous experiment was used to study the inhibition effect of the test materials on biofilm formation; quantification of biofilm formation was assessed as described by [27]. The optical density of each well was obtained by measuring the absorbance of each well at 600 nm using an ELISA microplate reader. The blank absorbance readings are used to determine the biofilm development of the isolates. Biofilm producers are the isolates whose OD values are more significant than the blank well. The cutoff value (ODc) can classify isolates as biofilm producers.

ODc: Average OD of negative control + (3 × standard deviation (SD) of negative control) …..(2)

OD isolate: Average OD of isolate – ODc…….. (3)

Classification of bacterial adherence based on OD values obtained for individual bacterial:

OD <= ODc (Non–adherent), 2ODc> OD> ODc (Weak), 4ODc> OD> 2ODc (Moderate), OD> 4 ODc (Strong).

However, 100 µl of test materials were provided. The plate was incubated for 24 hours at 37 °C. Then, all wells were rinsed, stained, and read at 600 nm with a microplate reader. Equation (4) estimated the percentage of biofilm inhibition. [28].

% Biofilm inhibition = $[(OD_{Control} - OD_{Sample})/OD_{Control}] \times 100$……(4)

Statistical analysis

The results were statistically calculated using Microsoft Excel 2019, one-way ANOVA, and p-value demonstrated on probability $P<0.05$ and the LSD for comparing the results.

Results

GC-MS analysis of SAE

Table 1 lists the chemical compositions of SAE determined by GC-MS, their retention time and percent of the composition area.

Compound	Retention Time Min.	%Area
Eugenol	13.118	77.53
Eugenol	14.148	3.30
Phenol, 2-methoxy-4-(2-propenyl)-acetate	15.860	12.71
Eugenol	16.645	3.54
trans-Isoeugenol	17.193	2.93

Table 1. Chemical composition of S. aromaticum extract.

The SAE contains (84.37%) eugenol, according to the results of GC-MS analysis, and three varied retention times were discovered. The three approaches' retention times are (13.118), (14.184), and (16.645) minutes, respectively. For eugenol, different retention times have been observed; this result is the same as reported by [29]. According to previous studies, eugenol is the primary chemical compound in SAE, which has different biological activities as an antioxidant, anti-carcinogenic, antimicrobial, antifungal, and insecticidal characteristics. This reflected the therapeutic effectiveness of SAE; these results agree with [30,31,32], who found that eugenol is the main compound in the SAE and has different biological activities.

Characterization of SACSNPs

UV-Visible spectroscopy

The absorbances of SAE and SACSNPs were measured, and the results are shown in tables (2); the decrease in the absorbance value at wavelength (542.00) nm from (0.024) in the SAE to (0.006) nm in SACSNPs, as well as the highest absorbance value at the wavelength (250.00) nm with a value of (1.806) in SACSNPs material after it was the highest value in SAE at a wavelength of (230.00) nm with a value of (1.534), in addition to the disappearance of the wavelength (230.00) nm in the SACSNPs and the appearance of a new wavelength with high absorbance at (250.00) in SACSNPs all, indicate the formation of the nanomaterial and the successful loading of the extract on chitosan nanoparticles.

Peak No.	wave-length nm	SAE	SACSNPs
1	542	0.024	0.006
2	357	0	0.369
3	277	1.177	0
4	250	0	1.806
5	230	1.534	0
6	204	0	0.169

Table 2. UV-Visible spectral analysis results of SAE and SACSNPs.

3.3. Fourier transformation infrared spectroscopy (FTIR)

FTIR analysis was employed to identify functional groups responsible for reducing Chitosan (CS) to SACSNPs and their stabilization. FTIR analysis was performed in the range of 400–4000 cm^{-1}. When comparing the spectra of CS and SACSNPs in the beginning, a new spectrum appeared at 449.41 cm^{-1} that was not present in CS, indicating the emergence of a new bond as a result of a new compound. In addition to comparing the spectra area, it was found in CS at the peak of 495.71 cm^{-1}, the area was 2.445, while in SACSNPs at the peak of 493.78 cm^{-1}, the area was 4.326, and at the central peak of the CS at 3393.79 cm^{-1} and its area 86,435 while in SACSNPs the central peak was 3132.4 cm^{-1} and with an area 224,511. This indicates that the large molecules were broken into smaller molecules, and when they are linked with chitosan, the value of the surface area of the bond increases, and the area increases. Changes in the functional groups of active biomolecules might indicate that they are related to forming SACSNPs. Figure 1 These results agree with [19, 33].

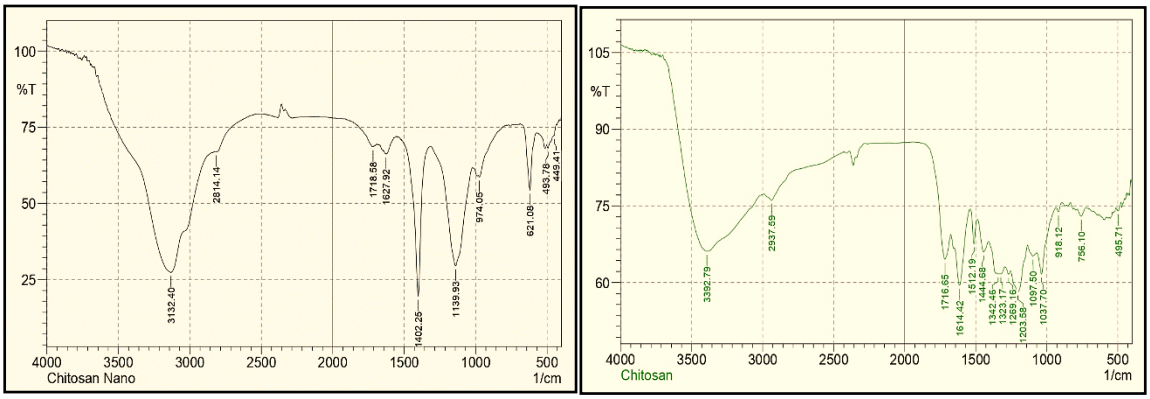

Figure 1. FTIR Spectra Pattern of Chitosan and Chitosan- nanoparticles.

Atomic force microscope analysis AFM

Atomic Force Microscopy images were used to measure particle sizes and the topography of the surface of SACSNPs; the size of particles obtained ranged from 26.74 to 53.96 nm. Figure 2 shows the distribution of SACSNPs according to the particle size.

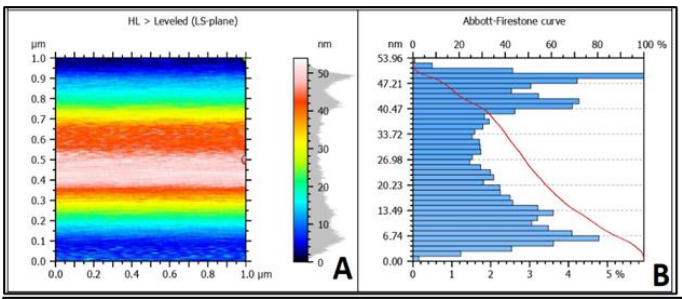

Statistical summary

Parameters	Unit	Mean	Std dev	Min	Max
Projected area	µm²	0.01818	0.09244	4.325e-06	0.4895
Z-maximum	nm	28.19	5.063	26.74	53.96

Figure 2. Distribution of SACSNPs according to particle size

Scanning Electron Microscope SEM

The morphology of SACSNPs was investigated using SEM; the results are presented in Figure 3. SACSNPs have a spherical appearance with a diameter range of 37.96-79.01 nm. and have a relatively homogeneous morphology. These results agreed with [20] that the resulted morphological mediated chitosan was exhibited with uniform particles, and their average size was 40–96 nm.

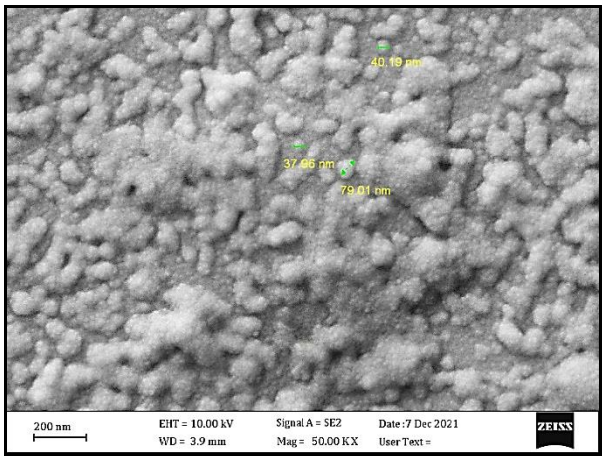

Figure 3. Scanning Electron Microscopy image of SACSNPs.

X-ray diffraction XRD

Figure 4A shows the X-ray diffraction patterns of chitosan, which shows the central peak of 2θ value at 20.53° and an intensity level close to 1200 cont. On the other hand, Figure 4B shows the SACSNPs peak, which shows its main peak of 2θ value at 22.8596° and an intensity level at 736.5503 cont. This change indicates the difference in the crystal structure between these two materials, where SACSNPs were more crystalline than chitosan.

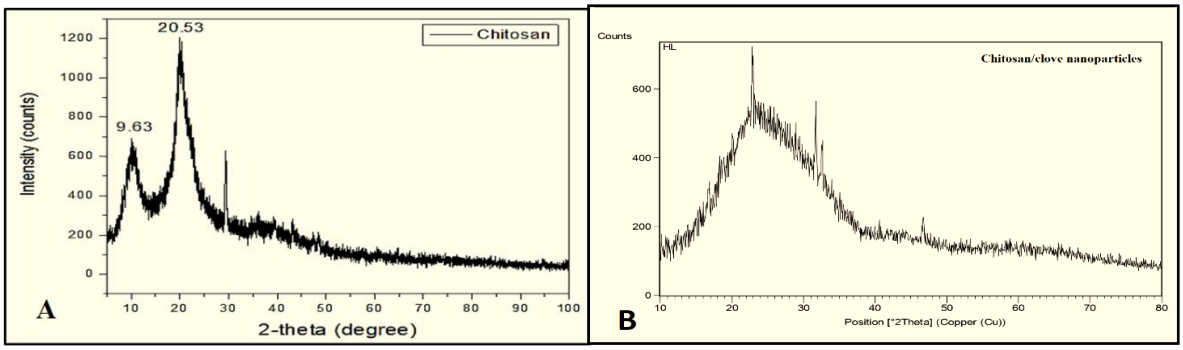

Figure 4 A. Diffractogram of Chitosan [34], (B) Diffractogram of SACSNPs.

Determination of eugenol concentration in analytical substances by HPLC

The concentration of eugenol was estimated by comparing the retention time and the area of SAE, as well as SACSNPs, with the standard eugenol, where eugenol is the primary active compound in the SAE [35]. The results were as follows:

The peak of standard eugenol 10 µg/ml was 8.30 min with an area of 325.06 Figure (5A). While for the SAE, it was observed that the peak of eugenol appeared at 8.22 min. With an area of 5897.66 (5B) and in the SACSNPs, it was 8.36 min with an area of 3566.25 Figure (5C). The concentrations are calculated according to equation (1) [18]. The results are listed in Table 3.

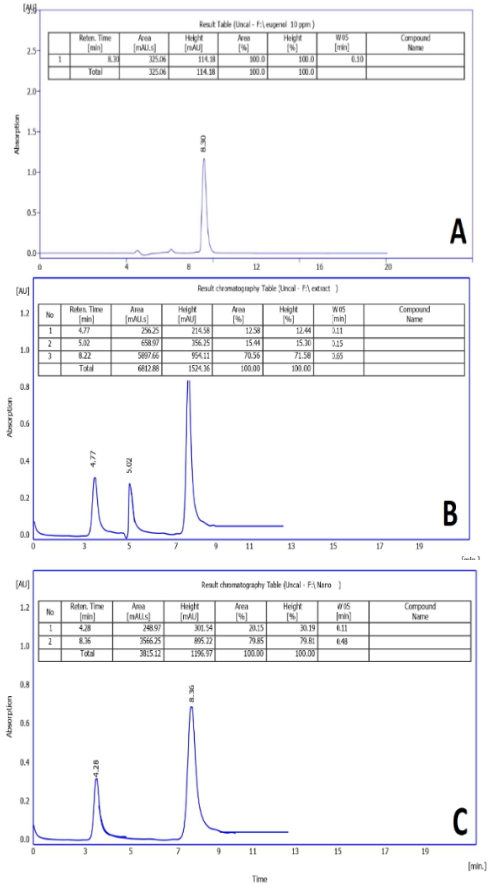

Figure 5. HPLC chromatogram of Eugenol in A: Standard 10µg/ml B: SAE C: SACSNPs.

NO.	Substance	Concentration (µg/ml)
1	Eugenol standard	10
2	*S. aromaticum* extract (SAE)	1209.6
3	SACSNPs	109.7

Table 3. The calculated concentrations of eugenol SAE and SACSNPs from HPLC results.

Identification of K. pneumonia

Culturing Examination

All fifty isolates were examined primarily for colony characterization by culturing on the selective media, CHROMagar, MacConkey agar, and blood agar. They were then incubated for 24 hours at 37ºC. The appeared colonies of K. pneumonia on CHROMagar resulted in the growth of mucoid metallic blue colonies, which refer to the presence of K. pneumonia spp. [25]. On MacConkey agar, pink, mucoid, lactose fermented colonies were considered Klebsiella spp. While colonies on blood agar, Greyish white, mucoid, and non-hemolytic colonies Figure (6) [36].

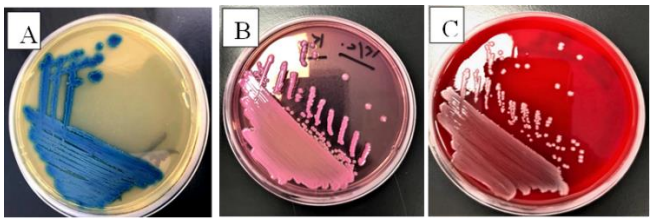

Figure 6. *K. pneumonia* on (A) CHROMagar, (B) MacConkey agar, (C) Blood agar.

Identification of K. pneumonia by Vitek-2 System

This system has been used in several previous research due to its success in identifying and confirming biochemical tests. The Vitek-2 compact was used to identify all 50 clinical isolates as K. pneumonia. It was demonstrated that the results of this system matched those of traditional tests. The analytical profile index of this system showed a 99.99% identification percentage probability of K. pneumonia.

Determination of Minimum Inhibitory Concentration using the MTP method

Since eugenol is the main active compound of SAE, which is attributed to most of the therapeutic activities, as well as represents 84.37 % of the crude SAE, according to the findings of GCMS analysis in this study see Table 1, the concentration of eugenol which was estimated by HPLC previously table 3 was approved to compare the MIC of SAE and SACSNPs.

The MIC and Sub-MIC values for test substances of K. pneumonia isolate compared to the controls. All of the wells were blue. After 2-4 hours of incubation, several wells' color changed to pink, suggesting bacterial development. The antibacterial activity of the SACSNPs was greater than that of the SAE, as evidenced by the color change with different concentrations in Figure 7 and Table 4.

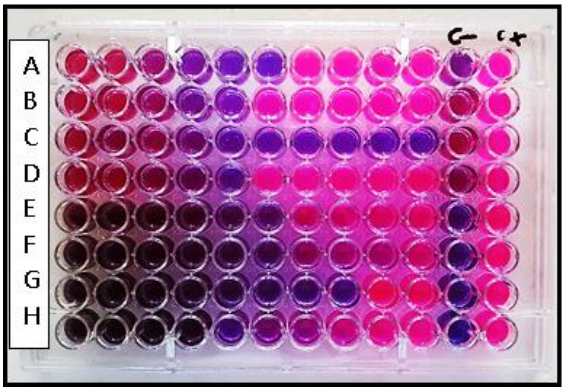

Figure 7. Microtiter plate 96-well of SACSNPs (A-D) and SAE (E-H) on *K. pneumonia*.

Isolates	SACSNPs MIC	SAE MIC	LSD	SACSNPs Sub-MIC	SAE Sub-MIC	LSD
K33	3.12	37.7	5.31 *	1.56	18.85	4.59 **
K35	6.25	37.7	6.44 *	3.12	18.85	5.02 **
K36	0.19	9.4	3.19 *	0.95	4.7	2.18 **
K37	6.25	75.5	7.03 *	3.12	37.7	5.93 **

K40	3.12	37.7	5.31 *	1.56	18.85	5.02 **
K41	6.25	37.7	6.44 *	3.12	18.85	5.02 **
K42	3.12	37.7	5.31 *	1.56	18.85	4.59 **
K46	6.25	9.4	2.91 *	3.12	4.7	1.89 NS
K47	6.25	75.5	7.03 *	3.12	37.7	5.82 **
K50	3.12	37.7	5.31 *	1.56	18.85	4.59 **
LSD	2.07 *	6.69 *	---	2.07 *	7.41**	---
*** (P≤0.05), ** (P≤0.01).**						

Table 4. The MIC and MBC by resazurin-aided microdilution method of SACSNPs and SAE on *K. pneumonia.*

When statistically analyzing and comparing the MIC values of the SAE and SACSNPs at (P≤0.05). There was a difference in the effectiveness of SAE and SACSNPs, indicating the presence of substantial variations between the two groups. The MIC for SAE varied from 75.7 to 37.7 µg/ml, while the MIC for SACSNPs ranged from 6.25 to 3.12 µg/ml. These were the optimal values for inhibiting K. pneumonia growth. On the other hand, the value of Sub-MIC was compared statistically and showed a highly significant difference between both SAE and SACSNPs at probability (P≤0.01). These results agree with previous studies by [37], who reported that chitosan nanoparticles can inhibit 50% to 84.8% of K. pneumonia in the concentration of (115, 161, 422, and 610 µg/ml) respectively.

Detection of Antimicrobial Efficacy of Substances Against Biofilm Production

For determining an agent's efficiency against biofilm development using a microplate reader. The impact of the test materials on the production or inhibition of biofilm of the studied K. pneumonia isolates that generate strong biofilm was investigated using the minimal inhibition concentrations of SAE and SACSNPs Table 5.

Isolates	% Inhibition SACSNPs	% Inhibition SAE	LSD
K33	33.173	11.818	6.94 *
K35	49.454	39.448	9.56 *
K36	50.716	39.828	9.03 *
K37	33.545	19.591	8.44 *
K40	30.629	23.232	8.21 *
K41	48.188	20.833	7.49 *
K42	60.345	1.328	10.35 *
K46	33.491	27.171	8.52 *
K47	66.584	44.327	8.22 *
K50	67.998	65.527	9.08 *
LSD	**8.71 ***	**9.04 ***	**---**
*** (P≤0.05).**			

Table 5. OD of SACSNPs & SAE Against Biofilm Production of *K. pneumonia* isolates.

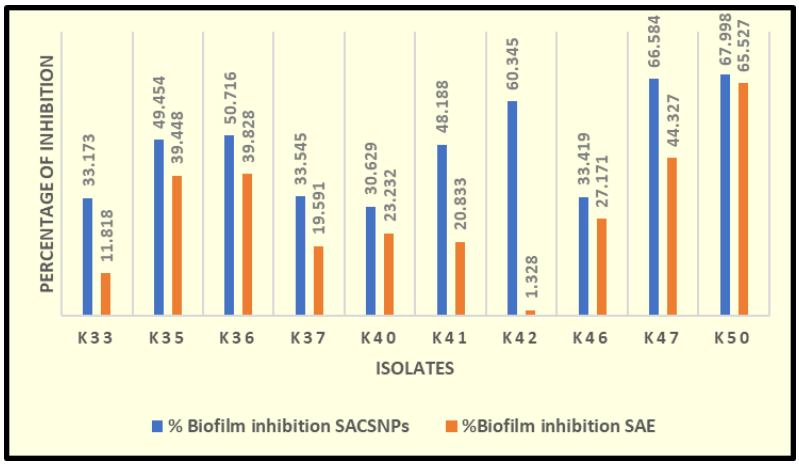

Figure 8. Percentage of inhibition of biofilm after being treated with Sub-MIC of SACSNPs and SAE.

The results demonstrate a considerable drop in optical density after treatment with experimental compounds. as seen in Figure (8). The SACSNPs show a vigorous inhibitory activity of 67.89 % and 65.02 %, respectively. Compared to the SAE, inhibitory activity against studied bacteria increased to 65.41 % and 41.72 %, respectively. The role of plant extract loaded with nanoparticles is that the Plant extracts work as both reducing and stabilizing agents. Phenolic and flavonoid chemicals are reducing agents, whereas amino acids function as stabilizing agents [38]. These properties lead to an increase in the activity of nanoparticles. The result shows that there were significant differences (P<0.05) between treatments (SAE and SACSNPs); SACSNPs were significantly better than SAE, which increased the inhibition percentage of biofilm produced by K. pneumonia. [20] proved that the essential oils were successfully loaded into the chitosan nanoparticles. It has more antibacterial activity against multi-drug-resistant K. pneumoniae.

Discussion

The electrostatic force between the SACSNPs and the bacterium cell wall promotes tighter contact with charged molecules, allowing SACSNPs to pass through the cell wall. Furthermore, CSNPs can alter the electron transport chain of bacteria [39]. Electrostatic interactions, which alter membrane permeability, are the most commonly suggested antibacterial activity of SACSNPs. It then attaches to DNA, preventing DNA replication and ultimately causing bacterial cell death. Furthermore, CSNPs have been found to penetrate cells, bind to DNA, and block the replication cycle [40]. [41] found that chitosan nanoparticles have more potent antibacterial activity due to Their unique characteristics, such as their more significant surface area and higher affinity with bacterial cells, which results in a quantum-size effect. 42 reported that The key finding of his work is that chitosan-alginate NPs are effective for treating Enterobacteriaceae infections.

Conclusions

A novel green strategy for generating antimicrobial nanoparticles was developed by chemically cross-linking two biomolecules to create a stable structure. Chitosan nanoparticles loaded with SAE were synthesized biologically with TPP as an across-linker. Based on the results of the current study, it was confirmed that the nano-chitosan loaded with S. aromaticum extract was a chemically stable substance with spherical particles of high crystallinity and grain size of up to 53

nm as a maximum, after conducting FTIR, UV-vis, AFM, SEM, XRD. The Sub-MIC of SACSNPs on the biofilm formation of Klebsiella pneumonia showed a significant effect on biofilm inhibition at a concentration of 3.12 µg/ml. In conclusion, we concluded that nano-chitosan loaded with alcoholic extract of SAE can inhibit biofilm production of Klebsiella pneumoniae isolated from urinary tract infections.

Acknowledgment

The authors extended their appreciation for the support of the Environmental and Water Directorate/Ministry of Sciences and Technology.

References

1. C. Caneiras, L. Lito, J. Melo-Cristino, and A. Duarte, "Community-and hospital-acquired Klebsiella Pneumoniae urinary tract infections in Portugal: Virulence and antibiotic resistance," *Microorganisms,* **2019***; 7(5),* pp. 1–14, doi: 10.3390/microorganisms7050138.
2. B. S. Rahal, A. A. Abdulhassan, N. Y. Salman, and K. Kassim, "The Role of EDTA in Biofilm Eradication of Klebsiella pneumoniae Isolated from Wound Infections," *Iraqi J. Biotechnol.,* **2021***; 20(1),* pp. 96–102.
3. N. Mamedov, "Medicinal Plants Studies: History, Challenges and Prospective," *Med. Aromat. Plants,* **2012***;01(08),* doi: 10.4172/2167-0412.1000e133.
4. S. Mickymaray, "Efficacy and mechanism of traditional medicinal plants and bioactive compounds against clinically important pathogens," *Antibiotics,* **2019***;8(4),* doi: 10.3390/antibiotics8040257.
5. S. Kaushal and K. Kaur, "Phytochemistry and pharmacological aspects of Syzygium aromaticum: A review K Kaur and S Kaushal," J. Pharmacogn. *Phytochem.,* **2019***; 8(1),* [Online]. Available: https://www.researchgate.net/publication/330215481.
6. S. Hussain, R. Rahman, A. Mushtaq, and A. El Zerey-pulaski, "Clove : A review of a precious species with multiple uses," *Int. J. Chem. Biochem. Sci.,* **2017***;11(1),* pp. 129–133.
7. S. Ali et al., "Journal Of Cancer Prevention Eugenol-Rich Fraction Of Syzygium Aromaticum (Clove) Reverses Biochemical And Histopathological Changes In Liver Cirrhosis And Inhibits Hepatic Cell Proliferation," *J Cancer Prev,* **2014***; 19,* Pp. 288–300, Doi: 10.15430/Jcp.2014.19.4.288.
8. J. K. Patra et al., "Nano-based drug delivery systems: Recent developments and prospects 10 Technology 1007 Nanotechnology 03 Chemical Sciences 0306 Physical Chemistry (incl. Structural) 03 Chemical Sciences 0303 Macromolecular and Materials Chemistry 11 Medical and He," *J. Nanobiotechnology,* **2018***; 16(1),* pp. 1–33, doi: 10.1186/s12951-018-0392-8.
9. M. Rofeal, F. Abdelmalek, and A. Steinbüchel, "Naturally-Sourced Antibacterial Polymeric Nanomaterials with Special Reference to Modified Polymer Variants," *Int. J. Mol. Sci.,* **2022***; 23(8),* p. 4101.
10. S. Moeinzadeh and E. Jabbari, "Nanoparticles and their applications," *Springer Handbooks,* **2017***; 9(1),* pp. 335–361, doi: 10.1007/978-3-662-54357-3_11.
11. M. Hadidi, S. Pouramin, F. Adinepour, S. Haghani, and S. M. Jafari, "Chitosan nanoparticles loaded with clove essential oil: Characterization, antioxidant and antibacterial activities," *Carbohydr. Polym.,* **2020**. *236,* p. 116075.
12. M. Yanat and K. Schroën, "Preparation methods and applications of chitosan nanoparticles; with an outlook toward reinforcement of biodegradable packaging," *React. Funct. Polym.,* **2020***; 161(12),* 2021, doi: 10.1016/j.reactfunctpolym.2021.104849.
13. M. A. Mohammed, J. T. M. Syeda, K. M. Wasan, and E. K. Wasan, "An overview of chitosan nanoparticles and its application in non-parenteral drug delivery," *Pharmaceutics,* **2017***; 9(4),* doi: 10.3390/pharmaceutics9040053.
14. B. Sultana, F. Anwar, and M. Ashraf, "Effect of extraction solvent/technique on the antioxidant activity of selected medicinal plant extracts," *Molecules,* **2009***;14(6),* pp. 2167–2180, doi: 10.3390/molecules14062167.

15. B. Amelia, E. Saepudin, A. H. Cahyana, D. U. Rahayu, A. S. Sulistyoningrum, and J. Haib, “GC-MS analysis of clove (Syzygium aromaticum) bud essential oil from Java and Manado,” *AIP Conf. Proc.*, **2017***; 1862(7)*, doi: 10.1063/1.4991186.
16. A. Nasti et al., “Chitosan/TPP and chitosan/TPP-hyaluronic acid nanoparticles: Systematic optimization of the preparative process and preliminary biological evaluation," *Pharm. Res.*, **2009***; 26(8)*, pp. 1918–1930, doi: 10.1007/s11095-009-9908-0.
17. S. Ngamsuk, T. C. Huang, and J. L. Hsu, “Determination of phenolic compounds, procyanidins, and antioxidant activity in processed coffee Arabica L. leaves," *Foods*, **2019***; 8(9)*, pp. 1–13, doi: 10.3390/foods8090389.
18. T. Kupiec, “Quality-control analytical methods: high-performance liquid chromatography.,” *Int. J. Pharm. Compd.*, **2004***;8(3)*, pp. 223–7, [Online]. Available: http://www.ncbi.nlm.nih.gov/pubmed/23924674.
19. M. Agarwal, M. K. Agarwal, N. Shrivastav, S. Pandey, R. Das, and P. Gaur, “Preparation of Chitosan Nanoparticles and their In-vitro Characterization,” *Int. J. Life-Sciences Sci. Res.*, **2018***; 4(2)*, pp. 1713–1720, doi: 10.21276/ijlssr.2018.4.2.17.
20. F. Zhang et al., "Antibacterial activity of chitosan loaded plant essential oil against multi-drug resistant K. pneumoniae," *Saudi J. Biol. Sci.*, **2020***; 27(12)*, pp. 3449–3455, 2020, doi: 10.1016/j.sjbs.09.025.
21. W. L. Du, Z. R. Xu, X. Y. Han, Y. L. Xu, and Z. G. Miao, “Preparation, characterization and adsorption properties of chitosan nanoparticles for eosin Y as a model anionic dye,” *J. Hazard. Mater.*, **2008***;153(1–2)*, pp. 152–156, doi: 10.1016/j.jhazmat.2007.08.040.
22. E. Atangana, T. T. Chiweshe, and H. Roberts, “Modification of Novel Chitosan-Starch Cross-Linked Derivatives Polymers: Synthesis and Characterization,” *J. Polym. Environ.*, **2019***; 27(5)*, pp. 979–995, doi: 10.1007/s10924-019-01407-0.
23. M. Anand, P. Sathyapriya, M. Maruthupandy, and A. Hameedha Beevi, “Synthesis of chitosan nanoparticles by TPP and their potential mosquito larvicidal application,” *Front. Lab. Med.*, **2018***; 2(2)*, pp. 72–78, doi: 10.1016/j.flm.2018.07.003.
24. CLSI, Performance Standards for Antimicrobial Susceptibility Testing, 31st ed. CLSI supplement M100. Wayne, PA: Clinical and Laboratory Standards Institute., **2021**.
25. Z. Samra, M. Heifetz, J. Talmor, E. Bain, and J. Bahar, "Evaluation of the use of a new chromogenic agar in detecting urinary tract pathogens," *J. Clin. Microbiol.*, **1998***; 36(4)*, pp. 990–994, doi: 10.1128/jcm.36.4.990-994.1998.
26. M. Elshikh et al., “Resazurin-based 96-well plate microdilution method for the determination of minimum inhibitory concentration of biosurfactants,” *Biotechnol. Lett.*, **2016***; 38(6)*, pp. 1015–1019, doi: 10.1007/s10529-016-2079-2.
27. E. F. Haney, M. J. Trimble, and R. E. W. Hancock, “Microtiter plate assays to assess antibiofilm activity against bacteria,” *Nat. Protoc.*, **2021***;16(5)*, pp. 2615–2632, doi: 10.1038/s41596-021-00515-3.
28. S. Shinde, L. H. Lee, and T. Chu, “Inhibition of biofilm formation by the synergistic action of EGCG-S and antibiotics,” *Antibiotics*, **2021**; *10(2)*, pp. 1–21, doi: 10.3390/antibiotics10020102.
29. N. Purwanti et al., “Emulsion stability of clove oil in chitosan and sodium alginate matrix,” *Int. J. Food Prop.*, **2018***; 21(1)*, pp. 566–581, doi: 10.1080/10942912.2018.1454946.
30. A. T. Zari, T. A. Zari, and K. R. Hakeem, “Anticancer Properties of Eugenol: A Review,” Molecules, vol. 26, no. 23, p. 7407, 2021.
31. M. Ulanowska and B. Olas, “Biological properties and prospects for the application of eugenol—a review,” *Int. J. Mol. Sci.*, **2021***; 22(7)*, doi: 10.3390/ijms22073671.
32. A. Ao et al., “Structure: Activity and Emerging Applications of Spices and Herbs,” **2021**.
33. J. G. Jabbar Almukhtar and F. F. Karam, “Preparation characterization and application of Chitosan nanoparticles as a drug carrier," *J. Phys. Conf. Ser.*, **2020***; 1664(1)*, doi: 10.1088/1742-6596/1664/1/012071.
34. S. Chandra Dey et al., "Preparation, Characterization and Performance Evaluation of Chitosan As an Adsorbent for Remazol Red,” Int. J. Latest Res. Eng. Technol., no. March, pp. 52–62, **2016**.
35. K. A. K. Mohammed, H. M. Abdulkadhim, and S. I. Noori, “Chemical Composition and Antibacterial Effects of Clove (Syzygium aromaticum) Flowers," *Int. J. Curr. Microbiol. Appl. Sci.*, **2016***; 5(2)*, pp. 483–489, doi: 10.20546/ijcmas.2016.502.054.

36. S. F. Klaif, H. H. Nasir, and J. N. Sadeq, "The genetic relationship for Klebsiella pneumoniae isolated from the human urinary tract and beef," *Iraqi J. Vet. Sci.,* **2018***;33(1),* pp. 75–80, doi: 10.33899/ijvs.2019.125531.1053.
37. P. R. Aguayo et al., "Antimicrobial and antibiofilm capacity of chitosan nanoparticles against wild type strain of pseudomonas sp. Isolated from cows' milk diagnosed with bovine mastitis," *Antibiotics,* **2020***; 9(9),* pp. 1–15, doi: 10.3390/antibiotics9090551.
38. R. Javed, M. Zia, S. Naz, S. O. Aisida, and Q. Ao, "Role of capping agents in the application of nanoparticles in biomedicine and environmental remediation: recent trends and prospects," *J. Nanobiotechnology,* **2020***; 18(1),* pp. 1–15.
39. A. Ivask et al., "Toxicity mechanisms in Escherichia coli vary for silver nanoparticles and differ from ionic silver." *ACS Nano,* **2014***; 8(1),* pp. 374–386, Jan, doi: 10.1021/nn4044047.
40. K. Birsoy, T. Wang, W. W. Chen, E. Freinkman, M. Abu-Remaileh, and D. M. Sabatini, "An Essential Role of the Mitochondrial Electron Transport Chain in Cell Proliferation Is to Enable Aspartate Synthesis.," *Cell,* **2015***;162(3),* pp. 540–551, Jul, doi: 10.1016/j.cell.2015.07.016.
41. M. Kong, X. G. Chen, K. Xing, and H. J. Park, "Antimicrobial properties of chitosan and mode of action: a state of the art review.," *Int. J. Food Microbiol.,* **2010***; 144(1),* pp. 51–63, Nov, doi: 10.1016/j.ijfoodmicro.2010.09.012.
42. W. N. Kadhum and I. A. Zaidan, "The Synergistic Effects of Chitosan-Alginate Nanoparticles Loaded with Doxycycline Antibiotic Against Multi-drug Resistant Proteus Mirabilis, Escherichia Coli and Enterococcus Faecalis," *Iraqi J. Sci.,* **2020***; 61(12),* pp. 3187–3199, doi: 10.24996/ijs.2020.61.12.6.

Received: May 15, 2023/ Accepted: June 10, 2023 / Published: June 15, 2023
Citation: Shaghati, H.A.; Jassim, EH; AL-Zubaidi, L.A.K. Biochemical Changes of Dexamethasone on Liver and Kidney functions in Laboratory Mice Mus musculus L. Revis Bionatura 2023;8 (1) 71.
http://dx.doi.org/10.21931/RB/CSS/2023.08.01.71